Analytical Methods

ROYAL SOCIETY OF CHEMISTRY

PAPER

View Article Online
View Journal | View Issue

Check for updates

Cite this: *Anal. Methods*, 2023, **15**, 3318

Stability and spectroscopic analysis of $CsPbBr_3$ quantum dots modified with 2-*n*-octyl-1-dodecanol

Hongyu Chen, [a] Mingshuo Liu,[a] Jianing Wang,[c] Yunfei Wang,[a] Yajuan Wang[a] and Wenyan Liu*[ab]

Received 11th April 2023
Accepted 9th June 2023

DOI: 10.1039/d3ay00542a

rsc.li/methods

Due to their excellent optical and electrical properties, all-inorganic metal halide perovskite $CsPbBr_3$ quantum dots (QDs) have become one of the most promising materials in the field of optoelectronics during recent years. However, the stability of $CsPbBr_3$ QDs limits their practical application and further development to a certain extent. In order to improve their stability, $CsPbBr_3$ QDs were modified with 2-*n*-octyl-1-dodecanol for the first time in this paper. The 2-*n*-octyl-1-dodecanol-modified $CsPbBr_3$ QDs were prepared by the ligand-assisted reprecipitation (LARP) method at room temperature in an air environment. Then the stability of the samples was tested at different temperatures and humidity. When the humidity was 80%, the photoluminescence (PL) intensity of both unmodified and modified $CsPbBr_3$ QDs increased to different degrees because the appropriate amount of water changed the crystallization environment. The PL intensity of the modified QDs increased, and the peak positions were basically not shifted, proving that they did not agglomerate. Thermal stability test results showed that the PL intensity of the 2-*n*-octyl-1-dodecanol-modified QDs could still maintain 65% of the original intensity at 90 °C, which is 4.6 times that of the unmodified $CsPbBr_3$ QDs. Experimental results show that the stability of $CsPbBr_3$ QDs is significantly improved after 2-*n*-octyl-1-dodecanol modification, which demonstrates the excellent surface passivation of $CsPbBr_3$ QDs by 2-*n*-octyl-1-dodecanol.

1. Introduction

With the continuous progress of human civilization, the energy consumption in the field of lighting and display is increasing, resulting in the over-exploitation of non-renewable energy, which causes the environmental pollution problem.[1,2] Dealing with this problem has become a difficult issue to be solved urgently.[3] Therefore, renewable energy and new photovoltaic materials have been developed and applied on a large scale in this context.[4,5]

As a direct band-gap semiconductor, perovskite materials have gradually emerged from the crowd of new optoelectronic materials and become a research hotspot in recent years due to their low preparation cost, high photoluminescence quantum yield (PLQY), narrow half-peak width of the emission spectrum, and tunable emission wavelength.[6–8] Among them, the quantum-limited effects of zero-dimensional all-inorganic cesium lead halide perovskite quantum dots (PQDs) have brought about infinite possibilities for their application in the field of luminescence.[6]

The research of all-inorganic PQDs has become mature and this material has shown excellent performance in the field of optoelectronics. However, stability is an important issue that has been restricting their further development. Since this material is extremely sensitive to water, light, heat, and air environments, long-term exposure to such environments is extremely prone to irreversible degradation.[9–11] In addition, the heavy metal element lead contained in this material will leak out with the degradation of the material, and cause serious impact on the surrounding environment and people.[12,13] On the other hand, PQDs are prone to agglomerate under the action of moisture and light and they will grow into larger crystal particles under an oxygen environment, which leads to a sharp decrease in PLQY. Therefore, finding a new scheme to stabilize the crystal structure of PQD materials is a necessary condition to promote this material to enter future optical applications.[14]

As reported previously, researchers have conducted extensive and in-depth studies on how to improve the efficiency and stability of all-inorganic PQDs. They proposed some strategies to improve their related properties, including but not limited to ligand modification, core–shell coating, doping, and other strategies.[15,16]

[a]*Department of Physics, School of Sciences, Beihua University, Jilin 132013, China. E-mail: wyliu1234@163.com*

[b]*Department of Materials Science and Engineering, Beihua University, Jilin 132013, China*

[c]*Changchun Institute of Optics, Fine Mechanics and Physics, Chinese Academy of Sciences, Changchun 130033, China*

In this study, we have innovatively proposed the modification of PQDs by introducing 2-*n*-octyl-1-dodecanol in the precursor solution. The introduction of a long alkyl chain as an organic functional group with strong hydrophobicity can effectively improve the water stability of the material. And the hydroxyl group has been confirmed in previous studies to produce hydrogen bonding interaction with halogen ions (X^-), which anchors the *ortho*-octahedral structure of $[PbX_6]^{4-}$ and reduces the probability of the PQD degradation. Moreover, the hydroxyl group is located at the end group of 2-*n*-octyl-1-dodecanol. After interacting with PQDs, a hydrophobic layer is formed on the surface, which greatly isolates the contact between QDs and water. Therefore, the introduction of 2-*n*-octyl-1-dodecanol can improve the overall stability of the PQDs and passivate the surface defects.

2. Results and discussion

To investigate the interaction between 2-*n*-octyl-1-dodecanol and PQDs, X-ray photoelectron spectroscopy (XPS) was conducted on the QDs before and after introducing 2-*n*-octyl-1-dodecanol. The test results are presented in Fig. 1.

Fig. 1a illustrates the full spectrum of XPS for the samples measured before and after introducing 2-*n*-octyl-1-dodecanol. It is evident that the positions of the characteristic peaks for both samples are almost identical. Fig. 1b–d display the characteristic peaks of Cs 3d, Pb 4f, and Br 3d, respectively. The figures demonstrate that after the introduction of 2-*n*-octyl-1-dodecanol, the positions of each characteristic peak shifted towards high binding energy. This transformation indicates that the introduced 2-*n*-octyl-1-dodecanol interacts with $CsPbBr_3$ QDs and increases the bond energy of each element, increasing its binding energy. According to Lewis acid–base neutralization theory, the –OH group in 2-octyl-1-dodecanol can effectively coordinate with the halogen vacancies in perovskite quantum dots and the free Pb^{2+} ions. This further reduces the surface defects of the perovskite quantum dots.[17–19]

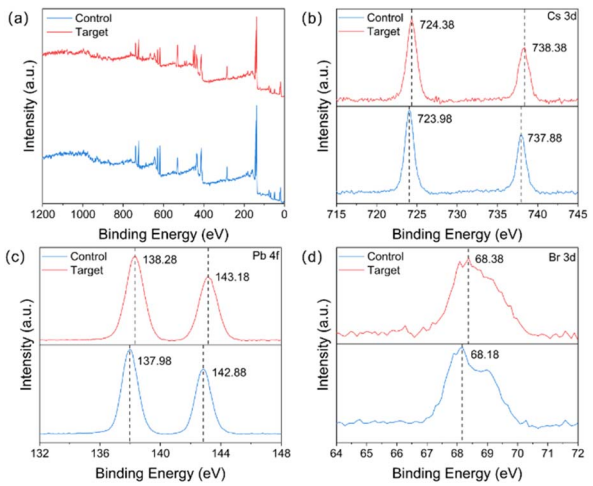

Fig. 1 XPS spectra of 2-*n*-octyl-1-dodecanol-modified and unmodified $CsPbBr_3$ QDs: (a) full spectrum, (b) Cs 3d, (c) Pb 4f, and (d) Br 3d.

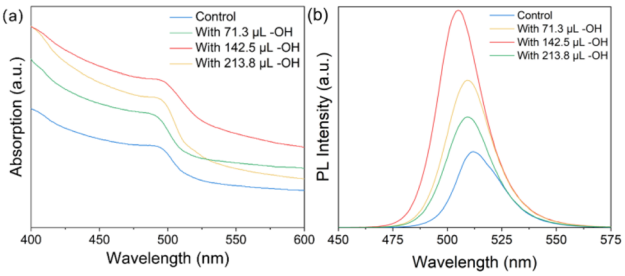

Fig. 2 UV-vis (a) and PL (b) of samples with different 2-*n*-octyl-1-dodecanol introduction quantities.

To investigate the impact of different concentrations of 2-*n*-octyl-1-dodecanol on the performance of $CsPbBr_3$ QDs, absorption and PL spectra were analyzed. Fig. 2a shows the absorption spectra of $CsPbBr_3$ QDs with varying amounts of 2-*n*-octyl-1-dodecanol. The figure indicates that 2-*n*-octyl-1-dodecanol introduction significantly enhances the absorption intensity of $CsPbBr_3$ QDs and that introducing 71.3 μL and 142.5 μL 2-*n*-octyl-1-dodecanol has no impact on the optical band gap. The introduction of 213.8 μL 2-*n*-octyl-1-dodecanol leads to an absorption peak mutation, demonstrating that an excessive amount of 2-*n*-octyl-1-dodecanol can alter the crystal structure of $CsPbBr_3$ QDs. The absorption intensity was highest at 142.5 μL 2-*n*-octyl-1-dodecanol. Fig. 2b illustrates the change in the PL intensity of $CsPbBr_3$ QDs after introducing various 2-*n*-octyl-1-dodecanol concentrations. It is evident that the PL intensity increases considerably following 2-*n*-octyl-1-dodecanol introduction, and the PL peak undergoes a blue shift when introducing 71.2 μL and 142.5 μL 2-*n*-octyl-1-dodecanol, indicating a decrease in the internal defect state density.[20,21] Specifically, the PL peak position undergoes a red-shift following the introduction of 213.8 μL 2-*n*-octyl-1-dodecanol, demonstrating that an excess of 2-*n*-octyl-1-dodecanol can affect the crystal structure.[22,23]

The figures in Fig. 3 illustrate the normalized UV-visible absorption spectrum (UV-vis) and the normalized PL of $CsPbBr_3$ QDs before and after modification with the optimal concentration of 2-*n*-octyl-1-dodecanol, which is 142.5 μL. The unmodified sample is labeled as control, and the modified sample is labeled as target. As mentioned in Fig. 3a, the introduction of 2-*n*-octyl-1-dodecanol did not significantly alter the absorption peak position, as it did not impact the optical band gap of $CsPbBr_3$ QDs.[24]

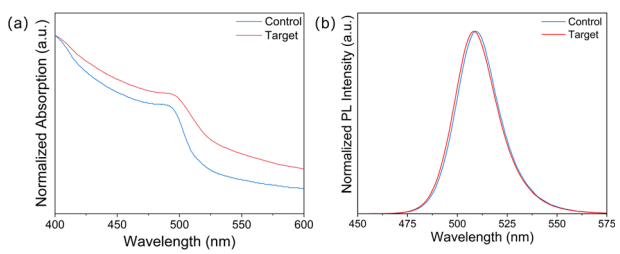

Fig. 3 UV-vis (a) and PL (b) spectra of dodecanol modified and unmodified $CsPbBr_3$ QDs.

However, the normalized PL spectra showed a significant blue shift, possibly due to the interaction between $CsPbBr_3$ QDs and 2-*n*-octyl-1-dodecanol.[25,26] This interaction enhanced the dielectric domain restriction effect in the system and reduced the density of defect states on the surface of QDs.[22,27] Despite the introduction of 2-*n*-octyl-1-dodecanol, the full width at half maxima (FWHM) of $CsPbBr_3$ QDs and 2-*n*-octyl-1-dodecanol-modified $CsPbBr_3$ QDs remained relatively similar, with FWHM values of 25 nm and 26 nm, respectively. This indicates that the introduction of 2-*n*-octyl-1-dodecanol did not cause excessive expansion of the FWHM, and the samples still maintained good monochromatic properties.[28]

Fig. 4a shows the FTIR spectra of $CsPbBr_3$ QDs modified with 2-*n*-octyl-1-dodecanol. It can be seen that the characteristic peaks of $CsPbBr_3$ QDs modified with 2-*n*-octyl-1-dodecanol appear close to 3414 cm^{-1}, 3415 cm^{-1} and 1626 cm^{-1}, which correspond to the symmetric stretching vibration of N–H bond and the antisymmetric stretching vibration of NH^+, respectively.[29] The characteristic peaks detected at 2857 cm^{-1}, 2851 cm^{-1}, 2927 cm^{-1}, and 2921 cm^{-1} correspond to the C–H stretching vibration of OA.[30] The characteristic peaks detected at 1458 cm^{-1}, 1462 cm^{-1}, 1396 cm^{-1}, and 1387 cm^{-1} correspond to the shear deformation vibration of CH_2 and the symmetric deformation vibration of CH_3, respectively.[31,32] In addition, for the FTIR spectra of the 2-*n*-octyl-1-dodecanol-modified QDs, a very distinct characteristic peak can be observed at 1006 cm^{-1}, which is attributed to the carbon–oxygen stretching vibration in 2-*n*-octyl-1-dodecanol.[33] The presence of C–O bonds indicates that 2-*n*-octyl-1-dodecanol is well dispersed in $CsPbBr_3$ QDs.[34] In order to investigate the crystal structure and crystallinity of the prepared samples, XRD characterization of $CsPbBr_3$ QDs and 2-*n*-octyl-1-dodecanol-modified $CsPbBr_3$ QDs was carried out separately, and the results are shown in Fig. 4b. It can be clearly observed in Fig. 4b that the characteristic diffraction peaks of $CsPbBr_3$ QDs appear at almost the same angle as those of $CsPbBr_3$ QDs after 2-*n*-octyl-1-dodecanol modification, indicating that the addition of 2-*n*-octyl-1-dodecanol did not change or destroy the structure of $CsPbBr_3$ QDs. Among them, the strong diffraction peaks appearing at 15.20°, 21.58°, 30.63°, 34.36°, 37.77° and 43.90° correspond to the cubic phase $CsPbBr_3$ (100), (110), (200), (210), (211) and (220) crystal planes, respectively (PDF # 00-054-0752). According to Lewis acid–base neutralization theory, the hydroxyl group in 2-octyl-1-dodecanol can react and neutralize the free lead ions and halogen vacancies in $CsPbBr_3$ quantum dots. As a result, it reduces the crystal defects and enhances the crystallinity of $CsPbBr_3$ quantum dots.[29,35]

Fig. 5 shows that the mean diameter of $CsPbBr_3$ QDs (Fig. 5a and c) and 2-*n*-octyl-1-dodecanol-modified $CsPbBr_3$ QDs (Fig. 5b and d) is approximately 22 nm and 18 nm, respectively. High-resolution transmission electron microscopy (HR-TEM) images in Fig. 5a and b indicate that the $CsPbBr_3$ QDs possess a cubic structure, while the sample modified with 2-*n*-octyl-1-dodecanol exhibits strong crystallinity, consistent with the XRD test results. Overall, the introduction of 2-*n*-octyl-1-dodecanol results in a reduction in the average size of PQDs and a more uniform distribution, as demonstrated in Fig. 5c and d.[24,36] This effect is attributed to the dielectric limit effect induced by introducing 2-*n*-octyl-1-dodecanol. In Fig. 5c and d illustrating the TEM images, the grain size distribution of PQDs is depicted.[37,38]

To further investigate the properties of $CsPbBr_3$ QDs, we conducted a study on their stability under high humidity conditions (80%) at the same temperature. Fig. 6 shows the PL spectra corresponding to different standing times. It can be observed from the figure that the PL intensity of QDs increases significantly with time, and its intensity increases to 178% of its initial value after standing for 150 minutes (Fig. 6a). This phenomenon is consistent with the reported observation that trace amounts of water can promote the crystallization of pure $CsPbBr_3$ QDs, as supported by our experimental results, which is consistent with our experimental results.[39]

However, we observed a slight decrease in the PL intensity after the unmodified QDs stood for 30 minutes. After 150 minutes, a stray peak appeared near the luminescence peak, and the peak wavelength of the PL spectra underwent a significant shift. These observations suggest that the stability of $CsPbBr_3$ QDs under higher humidity conditions deteriorates with increasing time.[40]

In contrast, in Fig. 6b, we observed that the PL intensity of the 2-*n*-octyl-1-dodecanol-modified $CsPbBr_3$ QDs increased with time, and the spectral curve was smooth and free of stray peaks.

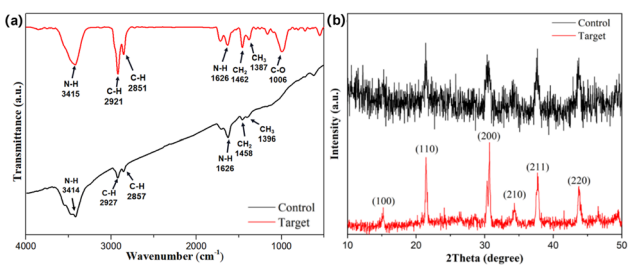

Fig. 4 FTIR spectra (a) and XRD spectra (b) of 2-*n*-octyl-1-dodecanol-modified and unmodified $CsPbBr_3$ QDs.

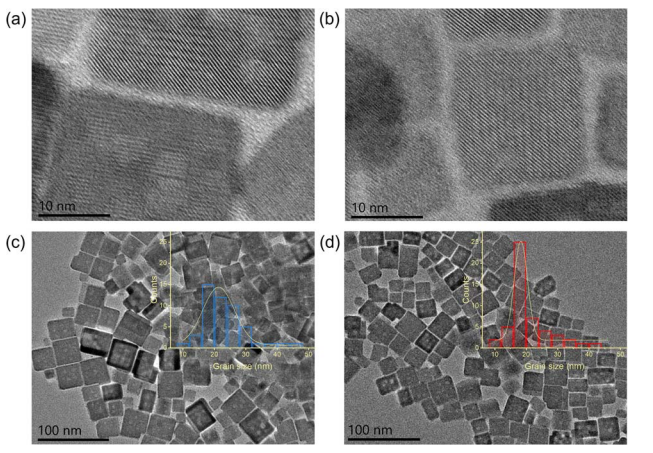

Fig. 5 HR-TEM (a and b) and TEM (c and d) of unmodified (a and c) and modified (b and d) $CsPbBr_3$ QDs with 2-*n*-octyl-1-dodecanol.

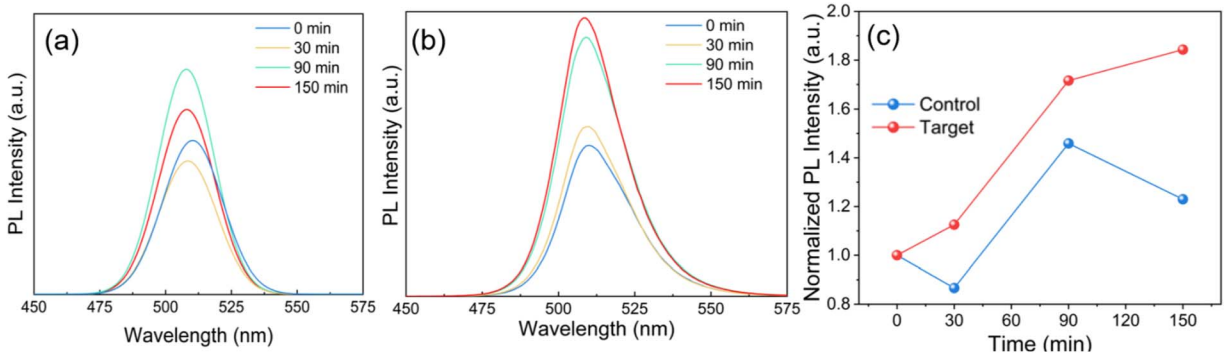

Fig. 6 PL intensity of unmodified (a) and modified (b) $CsPbBr_3$ QDs with 2-*n*-octyl-1-dodecanol changes with time under the same conditions (temperature and humidity), and (c) PL intensity change curve of (a) and (b).

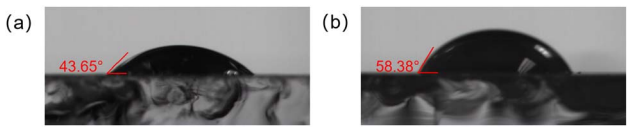

Fig. 7 Water contact angle of the film without (a) and with (b) 2-*n*-octyl-1-dodecanol.

Moreover, the peak position remained relatively stable, indicating that the modified $CsPbBr_3$ QDs did not agglomerate. The PL intensity at 150 minutes was 185% of the initial intensity, which is significantly higher than that of the unmodified QDs.

In summary, modifying $CsPbBr_3$ QDs with 2-*n*-octyl-1-dodecanol can greatly improve their water stability and protect their structure from damage. Our findings suggest that 2-*n*-octyl-1-dodecanol modification could have important practical applications in fields that require stable and high-performance $CsPbBr_3$ QDs.

According to previous studies, the long alkyl chains possessed by 2-*n*-octyl-1-dodecanol have certain hydrophobicity, which may be the reason for the improved stability of $CsPbBr_3$ QDs.[41,42] In order to further prove this inference, a water contact angle test was conducted for films with or without 2-*n*-octyl-1-dodecanol, and the results are shown in Fig. 7. The results showed that the water contact angle of the film with 2-*n*-octyl-1-dodecanol increased from 29.09° to 36.53° compared with the original film, which to some extent explained the enhanced hydrophobicity after the introduction of 2-*n*-octyl-1-dodecanol.

Fig. 8 shows the temperature-dependent PL spectra of $CsPbBr_3$ QDs unmodified and modified with 2-*n*-octyl-1-dodecanol. The temperature rises from 30 °C to 90 °C. The PL intensity of $CsPbBr_3$ QDs unmodified and modified with 2-*n*-octyl-1-dodecanol decreases significantly. This is may be due to the ligand (OA or OLA) from the quantum dot surface shedding or structural defects caused by high temperature.[43] As can be seen from Fig. 8a, the PL intensity of unmodified $CsPbBr_3$ QDs decreases with increasing temperature, dropping to about 21% and 15% of the original intensity at 70 °C and 90 °C, respectively. From the PL spectra of the 2-*n*-octyl-1-dodecanol-modified QDs (Fig. 8b), it can be seen that the PL intensity also decreases with increasing temperature. The PL intensity remains at about 69% of the original value at 90 °C, which is far higher than that of unmodified $CsPbBr_3$ QDs. Compared with Fig. 8a and b, it can be observed that the peak position of unmodified $CsPbBr_3$ QDs has a slight red-shift with increasing temperature.[44]

Meanwhile, the PL peak position gradually red-shifts with the increase of temperature, which may be caused by the increase of surface defect density caused by the shedding of ligands on the surface of QDs. This also proves that the modification of 2-*n*-octyl-1-dodecanol greatly improves the temperature stability of $CsPbBr_3$

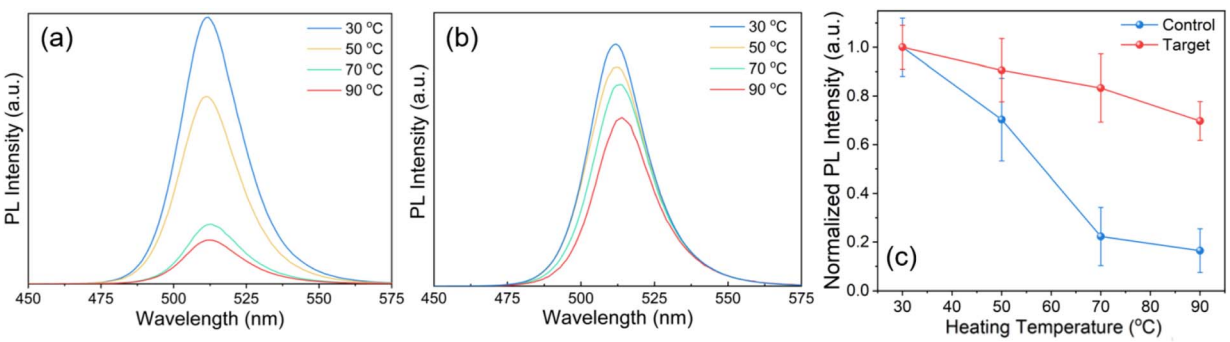

Fig. 8 PL intensity of unmodified (a) and modified (b) $CsPbBr_3$ QDs with 2-*n*-octyl-1-dodecanol changes with temperature from 30 °C to 90 °C, and (c) PL intensity change curve of (a) and (b).

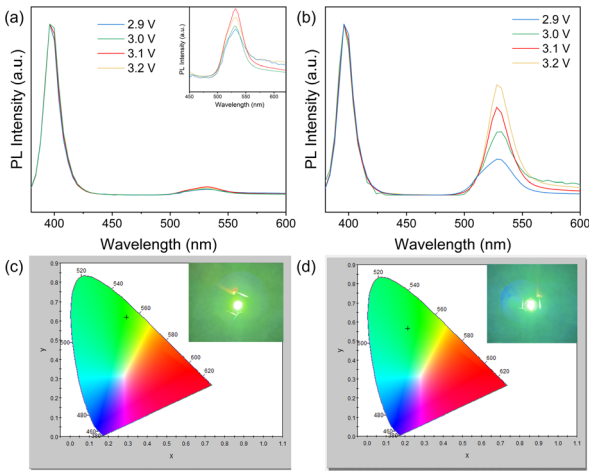

Fig. 9 PL intensity of a photoluminescence device: (a) control and (b) target. Chromaticity coordinate of $CsPbBr_3$ QDs with (c) and without (d) 2-*n*-octyl-1-dodecanol. The illustration is a real shot of the device.

QDs. In addition, the PL variation trend with temperature was plotted as a line graph to observe its stability performance better, as shown in Fig. 8c. The above data come from 5 sets of data in the same batch.

To further investigate the properties of 2-*n*-octyl-1-dodecanol modified samples, we prepared luminescent LED devices using $CsPbBr_3$ QDs before and after modification. Using a UV chip as the light source with an emission wavelength of 400 nm, we conducted tests on the LED devices. The test results, as shown in Fig. 9a and b, revealed a higher emission peak at 400 nm in the PL spectrum under different driving voltages (2.9–3.2 V), which is related to the excitation light source. The emission peak of $CsPbBr_3$ QDs was at 538 nm. It is noteworthy that, under the same driving voltage, the emission intensity of the modified sample was much higher than that of the original sample, indicating excellent performance of the modified sample in the luminescent LED device. Fig. 9c and d represent the color coordinates of the LED device, with the inseted image displaying the optical image of the prepared luminescent LED device. Fig. 9c shows the target sample and Fig. 9d shows the control sample.

3. Experimental

3.1. Materials

Cesium bromide (CsBr, 99.9%), lead(II) bromide ($PbBr_2$, 99.0%), oleic acid (OA, 90%), oleylamine (OLA, 90%), hexane (99%) and anhydrous ethanol (99.7%) were purchased from Aladdin Industrial Corporation, Shanghai, China. *N*,*N*-Dimethylformamide (DMF, 99.9%) was purchased from Sigma-Aldrich, Shanghai, China. 2-*n*-Octyl-1-dodecanol (>90.0%) was purchased from Aladdin Industrial Corporation, Shanghai, China. The above reagents were dehydrated with $K_nNa_{12-n}((AlO_2)_{12}(SiO_2)_{12})\cdot xH_2O$.

3.2. Preparation method of $CsPbBr_3$ QDs

In this paper, $CsPbBr_3$ QDs were prepared by the LARP method. 0.043 g CsBr and 0.073 g $PbBr_2$ were mixed into 5 mL DMF, 0.5 mL OA and 0.25 mL OLA to prepare the precursor solution. Next, the $CsPbBr_3$ QDs were synthesized by adding 1 mL of precursor into 10 mL of hexane. Then, 10 mL of anhydrous ethanol was added into the $CsPbBr_3$ QDs. The solution above was centrifuged at 6000 rpm for 6 min to obtain $CsPbBr_3$ QDs.

3.3. Preparation method of $CsPbBr_3$ QDs modified with 2-*n*-octyl-1-dodecanol

The preparation method is the same as that in 1.2, in which 142.5 μL of 2-*n*-octyl-1-dodecanol was added after the precursor was stirred to clarify.

3.4. Characterization

X-ray diffraction (XRD) maps were obtained by using an XRD-6100 (Cu Kα, Netherlands); absorption spectra were measured by using a UV-vis spectrophotometer (UV-2700, Germany); photoluminescence spectra were measured by using a fluorescence spectrophotometer (Omni PL-BH, China); a transmission electron microscope (JEM 2100F, Tokyo) and infrared spectrometer (iS50, USA) were used to perform transmission electron microscopy (TEM) and Fourier transform infrared spectroscopy (FT-IR). The elemental composition of the sample surface was tested by X-ray photoelectron spectroscopy (XPS, AXIS-Supra, Japan). The LED was tested using a portable spectroradiometer (PR-655, America).

4. Conclusions

In this paper, $CsPbBr_3$ QDs are synthesized by the LARP method and modified with 2-*n*-octyl-1-dodecanol to passivate surface defects and thus improve their stability. Compared with $CsPbBr_3$ QDs, the 2-*n*-octyl-1-dodecanol-modified $CsPbBr_3$ QDs exhibit better stability at high humidity and temperature. In water stability experiments, the 2-*n*-octyl-1-dodecanol modified QDs were more stable than the unmodified QDs and have higher PL intensity. Moreover, in thermal stability experiments, the PL intensity of unmodified QDs decreased substantially with increasing temperature, while the PL intensity of the 2-*n*-octyl-1-dodecanol-modified QDs decreased less, especially under high temperature conditions. The PL intensity of unmodified QDs decreased to about 21% of the original one at 70 °C, far less than that of QDs modified with 2-*n*-octyl-1-dodecanol, which still maintained a good luminescence effect at 90 °C. The results show that this method can provide a proven technical strategy to improve the stability of $CsPbBr_3$ QDs and other related issues and also provide some theoretical support for the application development of PQDs.

Author contributions

Chen Hongyu: conceptualization, writing – original draft, methodology and validation. Liu Mingshuo: investigation and formal analysis. Wang Yunfei: investigation and formal analysis. Liu Jianing: investigation, formal analysis, and funding acquisition. Liu Wenyan: writing – review & editing and funding acquisition.

Conflicts of interest

There are no conflicts to declare.

Acknowledgements

The authors would like to thank the National Natural Science Foundation of China, Grant (No. 61604003 and 62005268), Natural Science Foundation of Jilin Province (No. YDZJ202201ZYTS310), and Science and Technology Research Project of Department of Education, Jilin Province, China (No. JJKH20220044KJ).

References

1 V. Babin, P. Fabeni, M. Nikl, G. P. Pazzi, I. Sildos, N. Zazubovich and S. Zazubovich, *Chem. Phys. Lett.*, 1999, **314**, 31–36.
2 M. Kulbak, D. Cahen and G. Hodes, *J. Phys. Chem. Lett.*, 2015, **6**, 2452–2456.
3 A. Swarnkar, R. Chulliyil, V. K. Ravi, M. Irfanullah, A. Chowdhury and A. Nag, *Angew. Chem., Int. Ed.*, 2015, **54**, 15424–15428.
4 E. Yassitepe, Z. Yang, O. Voznyy, Y. Kim, G. Walters, J. A. Castaneda, P. Kanjanaboos, M. Yuan, X. Gong, F. Fan, J. Pan, S. Hoogland, R. Comin, O. M. Bakr, L. A. Padilha, A. F. Nogueira and E. H. Sargent, *Adv. Funct. Mater.*, 2016, **26**, 8757–8763.
5 Y.-F. Xu, M.-Z. Yang, B.-X. Chen, X.-D. Wang, H.-Y. Chen, D.-B. Kuang and C.-Y. Su, *J. Am. Chem. Soc.*, 2017, **139**, 5660–5663.
6 J.-H. Im, C.-R. Lee, J.-W. Lee, S.-W. Park and N.-G. Park, *Nanoscale*, 2011, **3**, 4088–4093.
7 L. Etgar, *Materials*, 2013, **6**, 445–459.
8 L. Etgar, P. Gao, P. Qin, M. Graetzel and M. K. Nazeeruddin, *J. Mater. Chem. A*, 2014, **2**, 11586–11590.
9 C. C. Stoumpos, C. D. Malliakas and M. G. Kanatzidis, *Inorg. Chem.*, 2013, **52**, 9019–9038.
10 Y. Shao, Z. Xiao, C. Bi, Y. Yuan and J. Huang, *Nat. Commun.*, 2014, **5**, 5784.
11 M. Hu, C. Bi, Y. Yuan, Y. Bai and J. Huang, *Adv. Sci.*, 2016, **3**, 1500301.
12 H. Zhu, Y. Pan, C. Peng, H. Lian and J. Lin, *Angew. Chem., Int. Ed.*, 2022, **61**, e202116702.
13 X. Ling, S. Zhou, J. Yuan, J. Shi, Y. Qian, B. W. Larson, Q. Zhao, C. Qin, F. Li, G. Shi, C. Stewart, J. Hu, X. Zhang, J. M. Luther, S. Duhm and W. Ma, *Adv. Energy Mater.*, 2019, **9**, 1900721.
14 L. Zhang, C. Kang, G. Zhang, Z. Pan, Z. Huang, S. Xu, H. Rao, H. Liu, S. Wu, X. Wu, X. Li, Z. Zhu, X. Zhong and A. K. Y. Jen, *Adv. Funct. Mater.*, 2021, **31**, 2005930.
15 Q. Wang, Y. Tong, M. Yang, H. Ye, X. Liang, X. Wang and W. Xiang, *J. Mater. Sci. Technol.*, 2022, **121**, 140–147.
16 Z. Zhang, L. Li, L. Liu, X. Xiao, H. Huang and J. Xu, *J. Phys. Chem. C*, 2020, **124**, 22228–22234.
17 L.-Q. Lu, T. Tan, X.-K. Tian, Y. Li and P. Deng, *Anal. Chim. Acta*, 2017, **986**, 109–114.
18 W.-C. Chen, Y.-H. Fang, L.-G. Chen, F.-C. Liang, Z.-L. Yan, H. Ebe, Y. Takahashi, T. Chiba, J. Kido and C.-C. Kuo, *Chem. Eng. J.*, 2021, **414**, 128866.
19 Z. Nie, L. Huang, C. Ren, X. Xiong, W. Zhu, W. Yang and L. Wang, *Mater. Chem. Phys.*, 2022, **275**, 125281.
20 C. Wu, D. Wang, Y. Chen, Z. Zhang, L. Wang, B. She, J. Xiong, W. Xie, Y. Huang and J. Zhang, *ACS Appl. Energy Mater.*, 2023, **6**, 2936–2944.
21 Y. Chen, D. Wang, Z. Zhang, B. She, L. Wang, C. Wu, J. Xiong, G. Zhu, W. Xie, Y. Huang and J. Zhang, *Energy Technol.*, 2023, **11**, 2201251.
22 Z. Dai, J. Chen and B. Yang, *J. Phys. Chem. Lett.*, 2021, **12**, 10093–10098.
23 Y. Liu, W. Chen, J. Zhong and D. Chen, *J. Eur. Ceram. Soc.*, 2019, **39**, 4275–4282.
24 A. T. Nomaan, A. A. Ahmed, N. M. Ahmed, M. I. Idris, M. R. Hashim and M. Rashid, *Ceram. Int.*, 2021, **47**, 12397–12409.
25 H. Guo, J. Liu, B. Luo, X. Huang, J. Yang, H. Chen, L. Shi, X. Liu, D. Benetti, Y. Zhou, G. S. Selopal, F. Rosei, Z. Wang and X. Niu, *J. Mater. Chem. C*, 2021, **9**, 9610–9618.
26 W. Zhou, Z. Zheng, Y. Lu, M. Sui, J. Yin and H. Yan, *RSC Adv.*, 2021, **11**, 20423–20428.
27 M. A. Padhiar, M. Wang, Y. Ji, Z. Yang and A. S. Bhatti, *Nanotechnology*, 2022, **33**, 175202.
28 F. Zhang, J. Song, B. Cai, X. Chen, C. Wei, T. Fang and H. Zeng, *Sci. Bull.*, 2021, **66**, 2189–2198.
29 J. Li, J. Chen, L. Xu, S. Liu, S. Lan, X. Li and J. Song, *Mater. Chem. Front.*, 2020, **4**, 1444–1453.
30 Y. Gao, X. Su, J. Zhang, H. Tan, J. Sun, J. Ouyang and N. Na, *Small*, 2021, **17**, 2103773.
31 B. Wang, B. Li, T. Shen, M. Li and J. Tian, *J. Energy Chem.*, 2018, **27**, 736–741.
32 N. Li, X. Chen, J. Wang, X. Liang, L. Ma, X. Jing, D.-L. Chen and Z. Li, *ACS Nano*, 2022, **16**, 3332–3340.
33 C. Wang, H. Lin, Z. Zhang, Z. Qiu, H. Yang, Y. Cheng, J. Xu, X. Xiang, L. Zhang and Y. Wang, *J. Eur. Ceram. Soc.*, 2020, **40**, 2234–2238.
34 L. Mao, Y. Wu, C. C. Stoumpos, M. R. Wasielewski and M. G. Kanatzidis, *J. Am. Chem. Soc.*, 2017, **139**, 5210–5215.
35 J. Chen, D. Liu, M. J. Al-Marri, L. Nuuttila, H. Lehtivuori and K. Zheng, *Sci. China Mater.*, 2016, **59**, 719–727.
36 P. Kumar, S. Mulmi, D. Laishram, K. M. Alam, U. K. Thakur, V. Thangadurai and K. Shankar, *Nanotechnology*, 2021, **32**, 485407.
37 F. Sui, M. Pan, Z. Wang, M. Chen, W. Li, Y. Shao, W. Li and C. Yang, *Sol. Energy*, 2020, **206**, 473–478.
38 S. S. Bhosale, E. Jokar, Y.-T. Chiang, C.-H. Kuan, K. Khodakarami, Z. Hosseini, F.-C. Chen and E. W.-G. Diau, *ACS Appl. Energy Mater.*, 2021, **4**, 10565–10573.
39 X. Zhang, X. Bai, H. Wu, X. Zhang, C. Sun, Y. Zhang, W. Zhang, W. Zheng, W. W. Yu and A. L. Rogach, *Angew. Chem., Int. Ed.*, 2018, **57**, 3337–3342.
40 Y.-T. Hsieh, Y.-F. Lin and W.-R. Liu, *ACS Appl. Mater. Interfaces*, 2020, **12**, 58049–58059.

41 M. H. Azar, M. Mohammadi, N. T. Rezaei, S. Aynehband, L. Shooshtari, R. Mohammadpour and A. Simchi, *ACS Appl. Nano Mater.*, 2021, **4**, 7788–7799.
42 H. Luo, Y. Huang, H. Liu, B. Zhang and J. Song, *Chem. Eng. J.*, 2022, **430**, 132790.
43 Y. Shu, Y. Wang, J. Guan, Z. Ji, Q. Xu and X. Hu, *Anal. Chem.*, 2022, **94**, 5415–5424.
44 A. E. Shalan, E. Akman, F. Sadegh and S. Akin, *J. Phys. Chem. Lett.*, 2021, **12**, 997–1004.

